IEEE Access
Multidisciplinary | Rapid Review | Open Access Journal

Received February 15, 2020, accepted March 9, 2020, date of publication March 23, 2020, date of current version April 10, 2020.

Digital Object Identifier 10.1109/ACCESS.2020.2982510

Modified WCA-Based Adaptive Control Approach Using Balloon Effect: Electrical Systems Applications

TAREK HASSAN MOHAMED[1], HUSSEIN ABUBAKR[1], MOHAMED ABDELHAMID MOHAMED ALAMIN[2], AND AMMAR MOSTAFA HASSAN[3]

[1]Department of Electrical Engineering, Faculty of Energy Engineering, Aswan University, Aswan 81528, Egypt
[2]Egyptian Hydro Power Generation Company, Aswan 81521, Egypt
[3]College of Computing and Information Technology, Arab Academy for Science, Technology and Maritime Transport, Aswan 81516, Egypt

Corresponding author: Ammar M. Hassan (ammar@aast.edu)

ABSTRACT This paper suggests an adaptive control approach using water cycle algorithm optimization method (WCA) modified by a new technique called ''Balloon Effect''. The main concept of Balloon Effect is to increase the ability of the WCA to tune individually the gains of the controller online. The proposed technique has been used to tune the gains of PID controller and applied to control both of the load frequency control in micro-grid power system (which minimize the fundamental frequency variations) and the position of armature-controlled DC motor. Digital simulations have been carried out to prove the efficiency of the proposed adaptive controller-based WCA with Balloon Effect. The obtained results showed that the proposed adaptive controller maintains robust performance, and effectively reduces the impact of identified disturbances and uncertainties.

INDEX TERMS Load frequency control, speed control of DC motor, adaptive control, water cycle algorithm, balloon effect.

I. INTRODUCTION

Despite modern and intelligent control techniques which appeared during last decades, PID controller acts as a main player to control the industrial and practical process. It has several advantages such as: simplicity, reliability and low cost [1]–[3].

One of the disadvantages of the fixed parameters PID controller is its low sensitivity to the process's parameters variations and system disturbance. An adaptive control is the control method used by a controller that adapts the parameters of the controller according to system parameters variations [4]. Also, many robust, optimal and intelligent control approaches have been discussed as load frequency controllers [5]–[9].

The adaptive control techniques have been applied to tune PID' gains according to the situation of the process. Myriad adaptive approaches have been introduced such as model reference adaptive control, model identification adaptive control and adaptive control with multiple models. Recently, there are some attempts to apply optimization approaches to tune the control parameters, this is because of their ability to deal with uncertainties and disturbances [10]–[14].

Optimization techniques have been used to make off-line tune of the classical PI-LFC such as in [15], [16]. Also, there are some attempts to use optimization methods to make an on-line tuning of adaptive LFC' parameters [17], [18].

On the other hand, WCA has been considered a meta-heuristics optimization technique. One of the advantages of WCA is its requirement of lower number of insensitive users, also, WCA can be applied in wide range of optimization issues using defined user fixed parameters [19]–[23].

One of the weaknesses of the classic WCA application in the adaptive control problem can be expressed as follows: according to the nominal transfer function of the plant considering no load disturbance, the objective function has been designed. Therefore, poor performance may occur at the moment of load disturbance and in the case of variations of the system parameters.

The Balloon Effect has been designed to make the optimization technique more sensitive to the variations that affect the system, such as load variation and changes in the system

The associate editor coordinating the review of this manuscript and approving it for publication was Utku Kose.

parameters. It represents the effect of the system changes on the on-time system open loop transfer function, which is similar to the effect of air on balloon size.

This paper suggested a modified WCA with Balloon Effect, this Balloon Effect (BE) is designed to enable WCA to work individually as an adaptive controller to tune the PID controller, by other way it increases the sensitivity of WCA to system parameters changes and system disturbance. An adaptive controller-based proposed WCA + BE has been applied to two applications: position control of DC motor and frequency control in micro-grid power system.

The contributions of this work can be outlined as follows:

- A novel modification for WCA optimization techniques named ''Balloon Effect'' has been presented for adaptive tuning of controller gain's parameters.
- Balloon Effect has been introduced with WCA technique for Electrical Systems' Applications such as adaptive frequency control in micro-grids and adaptive position control of DC motors.

The rest of the paper is organized as follows: Section II defines the main problem formulation. Sections III and IV illustrate the general overview of WCA and the main idea of the BE respectively. Robustness and stability of proposed scheme are presented in Section V. Applications of micro-grid system and dynamic model of the suggested system are discussed in details in Section VI In Section VII a modified WCA based frequency control is described. Section VIII shows the simulation results and discussions of the proposed controlled systems. Section IX shows the position control of DC motor applications and a modified (WCA + BE) based adaptive PV controller is described. Finally, Section X concludes the work and suggests some directions for future studies.

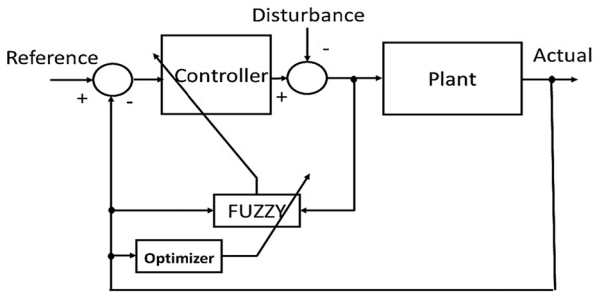

FIGURE 1. General scheme of the online optimizer-Fuzzy controller.

II. PROBLEM FORMULATION

Many publications utilized different optimization methods with such fuzzy controller as adaptive controller [17], [24], [25]. The main goal is limited to adjust the parameters of fuzzy controllers as shown in Fig. 1. On the other hand as shown in Fig. 1, this scheme is complicated and time consuming, since there is a huge calculation in both optimizer and fuzzy controller so that some attempts to use optimization method directly to tune PID controller to make the controller faster [26]–[28] as shown in Fig. 2.

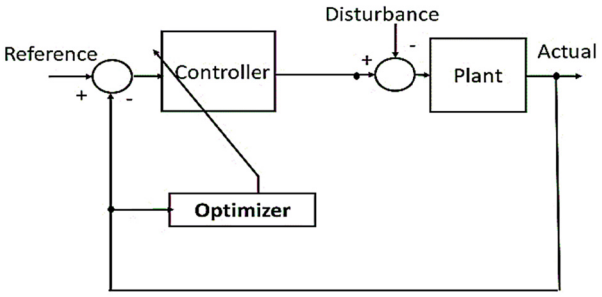

FIGURE 2. General scheme of adaptive controller based only optimizer.

III. GENERAL OVERVIEW OF WCA ALGORITHM

WCA is a mathematical representation of the physical natural water cycle [23]. The cycle story of how the streams and rivers flow to the sea is shown in Fig. 3.

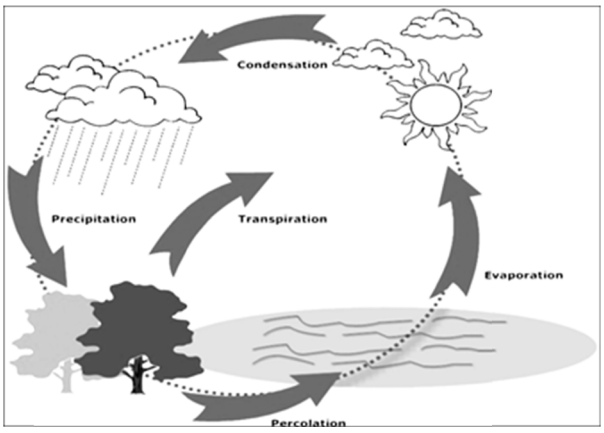

FIGURE 3. Simplified water cycle mechanism.

The initial population is assumed to design the variables that are divide into seas and rivers. The stream (using cost function) judges between solutions: best solution is the sea then the other best represents the river and the number of rivers is selected by the designer after that the other solutions for streams which flow to the river or the sea that is determined by NS factor. The movement of streams and rivers as shown in Fig. 4. [19]–[21].

A. OUTLINES OF WCA PROCEDURES AND STEPS CAN BE CONCLUDED AS FOLLOW

Step 1: Choose the initial parameters of the WCA: Nsr, Npop, dmax, Max. Iteration.

Step 2: The algorithm begin with generation of random initial population then form the initial rain drops(streams), sea, and rivers by cost function as shown in

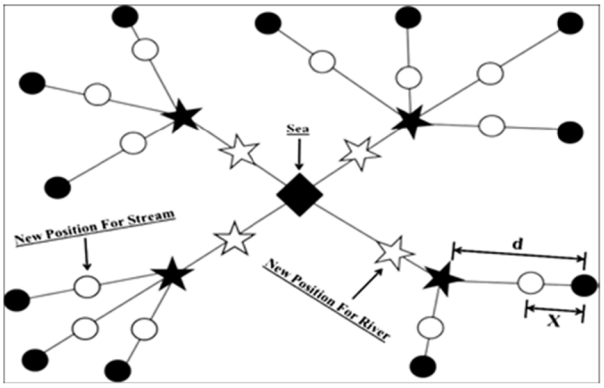

FIGURE 4. Schematic of WCA algorithm.

Eq. (1),(2), and (3) respectively.

$$pop\ of\ raindrop = \begin{bmatrix} raindrop1 \\ raindrop2 \\ \vdots \\ raindrop_{Npop} \end{bmatrix} = \begin{bmatrix} x_1^1 & x_2^1 & \cdots & x_{Nvar}^1 \\ x_1^2 & x_2^2 & \cdots & x_{Nvar}^2 \\ \vdots & \vdots & \vdots & \vdots \\ x_1^{Npop} & x_2^{Npop} & \cdots & x_{Nvar}^{Npop} \end{bmatrix} \quad (1)$$

where: $raindrop = [x_1, x_2, x_3, \ldots x_n]$

$$Cost_i = f\left(x_1^i, x_2^i, \ldots x_{Nvar}^i,\right) \quad i = 1, 2, 3, \ldots, N_{pop} \quad (2)$$

$$N_{sr} = number\ of\ river + \underbrace{1}_{sea} \quad (3)$$

Step3: Determine the number of streams that flow to the specific rivers or sea using:

$$NS_n = round\left\{\left|\frac{Cost_n}{\sum_{i=1}^{N_{sr}} Cost_i}\right| * N_{raindrops}\right\} n = 1, 2, \ldots, N_{sr} \quad (4)$$

Step 4: The stream will have a new position by flowing to the rivers, the new position will be compared to old position and the best solution will be replaced by:

$$X_{stream}^{i+1} = X_{stream}^i + rand * C * \left(X_{river}^i - X_{stream}^i\right) \quad (5)$$

Step 5: The step 2 is repeated but the new position of the stream is flowing to the river by Eq. (6).

$$X_{stream}^{i+1} = X_{stream}^i + rand * C * \left(X_{sea}^i - X_{stream}^i\right) \quad (6)$$

Step 6: Rivers flow to the sea that is the steepest place using Eq. (7).

$$X_{river}^{i+1} = X_{river}^i + rand * C * \left(X_{sea}^i - X_{river}^i\right) \quad (7)$$

Step 7: In this step, the evaporation condition tests the final position of the all streams with Eq. (8). If the evaporation condition is satisfied, the raining process will occur using Eq. (9).

$$\left|X_{sea}^i - X_{stream}^i\right| < d_{max} \quad i = 1, 2, 3, \ldots N_{sr} - 1 \quad (8)$$

$$X_{stream}^{new} = X_{sea} + \sqrt{\mu} * randn\,(1, N_{var}) \quad (9)$$

where: $\mathbf{d_{max}}$ is a small number (close to zero). Therefore, if the distance between a river and the sea is less than d_{max}, it indicates that the river has reached/joined the sea, and $\boldsymbol{\mu}$ is a coefficient that shows the range of searching region near the sea. **randn** is the normally distributed random number.

Step 8: Reduced the value of d_{max}, which is user defined parameter using:

$$d_{max}^{i+1} = d_{max}^i - \frac{d_{max}^i}{max\ iteration} \quad (10)$$

Step 9: Check the convergence criteria. If the stopping criterion is satisfied, the algorithm will stop, otherwise return to step 8. Finally, for all previous steps and procedures: The flowchart of WCA is shown in Fig. 5.

IV. GENERAL IDEA OF BALLOON EFFECT FOR OPTIMIZATION TECHNIQUES

BE is firstly suggested in [39] to control the position of a cart moved by a DC motor, also it is applied in LFC application in [40]. At any iteration, the objective function depends only on the value of the controller' gains [28]. This means that there is no direct effect of system changes on the objective function, and this leads to weak reaction of the optimizer in case of system issues. Balloon Effect (BE) has been designed to treat this point. 'Balloon Effect' carries the mean of the system changes effect on the value of the optimization' objective function and consequently on the performance of the optimization method itself. Fig. 6 shows the block diagram of any optimizer techniques supported by Balloon Effect as an adaptive integral control system.

The idea of Balloon effect when applied to optimization techniques is illustrated in Fig. 7. It can be noted that: at any iteration-i, main output $Y_i(S)$ and input $U_i(S)$ will be fed to the optimizer to calculate the actual process transfer function at this moment i as:

$$\boldsymbol{G_i}\,(\boldsymbol{S}) = \tilde{\boldsymbol{G}} = \frac{\boldsymbol{Y_i(S)}}{\boldsymbol{U_i(S)}} \quad (11)$$

In addition, $G_i\,(S)$ can be represented by its past value $G_{i-1}\,(S)$ as:

$$G_i\,(S) = AL_i \cdot G_{i-1}\,(S) \quad (12)$$

$\boldsymbol{AL_i}$ is a gain, and $G_{i-1}\,(S)$ can be expressed using the nominal process transfer function $G_0\,(S)$ as:

$$G_{i-1}\,(S) = \rho_i \cdot G_0\,(S) \quad (13)$$

where

$$\rho_i = \prod_{n=1}^{i-1} \mathrm{AL}_n \quad (14)$$

So, from (12) and (13) it can be noted that:

$$G_i\,(S) = AL_i.\rho_i \cdot G_0\,(S) \quad (15)$$

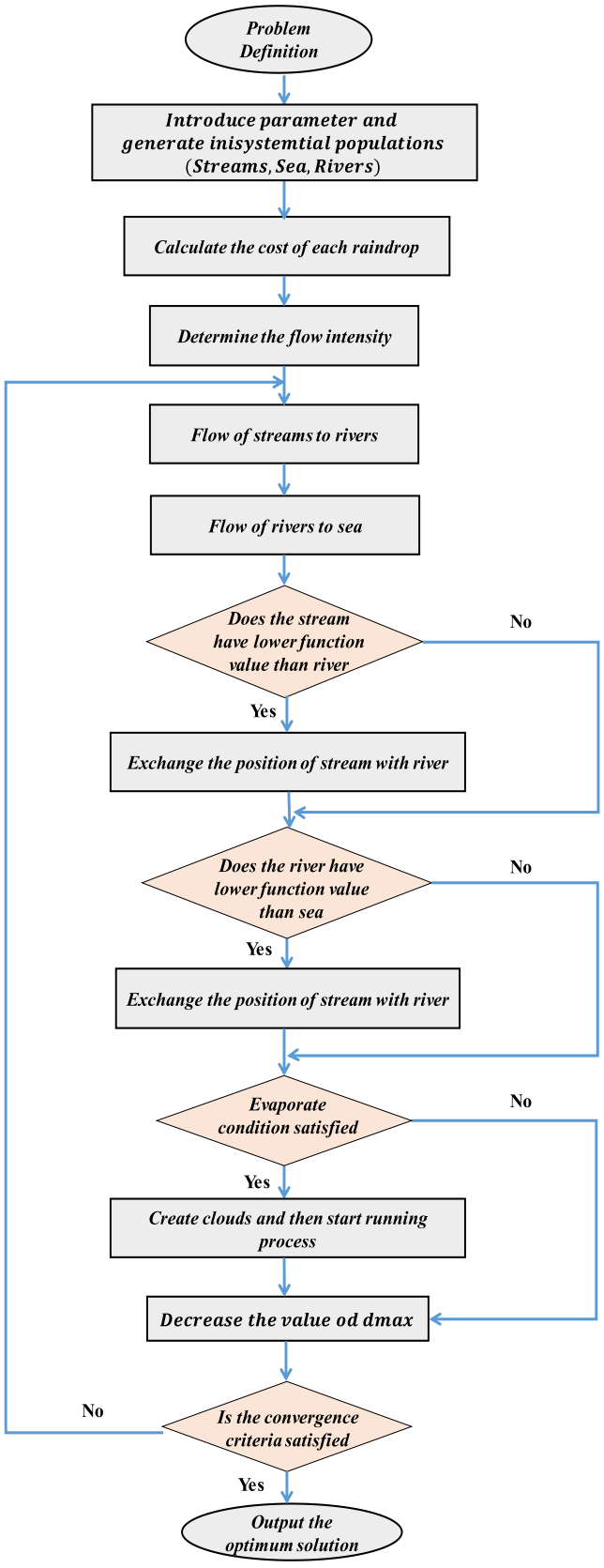

FIGURE 5. The standard flowchart of WCA algorithm [23].

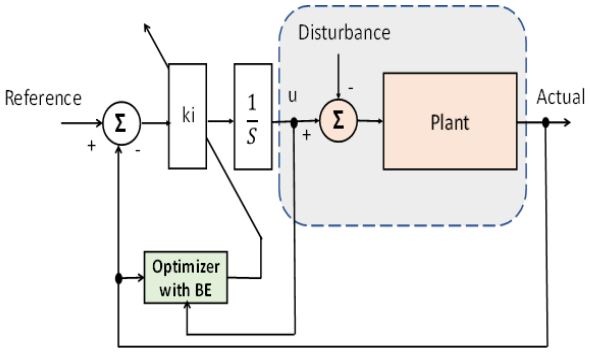

FIGURE 6. Micro-grid model based adaptive control system supported by BE.

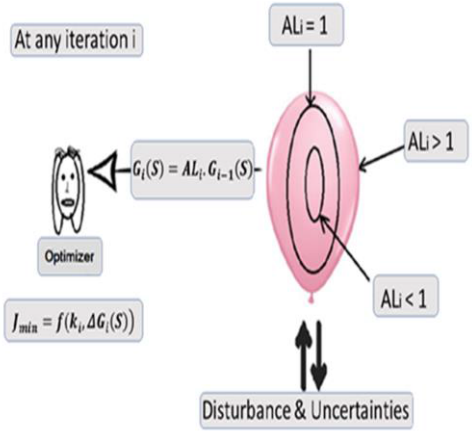

FIGURE 7. Idea of Balloon Effect for optimization methods at any iteration i.

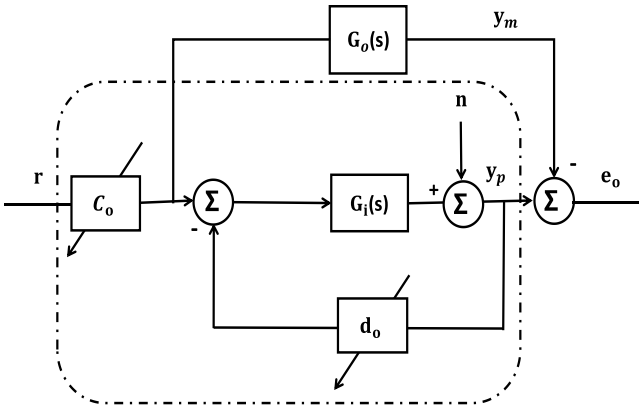

FIGURE 8. System' block diagram for stability [31].

Expression of 'Balloon Effect' is driven from that reality: the effect of system difficulties such as the disturbance and parameters uncertainties on $\mathbf{G_i}$ (**S**) resembles the effect of the air in/out on the balloon size. As a result of this effect, the objective function of the optimization technique at any iteration (**i**) will depend on the gains values and change in the value of $\mathbf{G_i}$ (**S**).

V. STABILITY AND ROBUSTNESS OF SUGGESTED WCA + BE SCHEME

The block diagram shown in Fig. 8 expresses the system with suggested controller, and it can be expressed as:

$$\left.\begin{aligned}\dot{X}_p &= A_p X_p + b_p c_0^* r \\ y_p &= C_p^T X_p\end{aligned}\right\} \tag{16}$$

where c_0^* is the nominal value of the feedforward controller's gain. The regress or w can be expressed as [29]–[31]:

$$w = w_m + Qe + q_n n \tag{17}$$

$Qe = \begin{bmatrix} 0 \\ y_p^* \end{bmatrix}$ is matrix of the error, n is the output noise

$$q_n^T = \begin{bmatrix} 0 & 1 \end{bmatrix} \in \left(\mathfrak{R}, \mathfrak{R}^{n-1}, \mathfrak{R}, \mathfrak{R}^{n+1}\right) = \mathfrak{R}^{2n}.$$

Considering the plant with nominal transfer function has been used as the base of the suggested adaptive controller, so the system output will be defined as:

$$y^* = G_0(S). \tag{18}$$

The actual output will be calculated as:

$$y(t) = y^* + H_a.u(t) \tag{19}$$

$$H_a = G_i(S) - G_0(S) \tag{20}$$

Assuming that H_a is an operator which satisfying that:

$$\|H_a \cdot u(t)\|_\infty \leq \gamma_a \|u(t)\|_\infty + \beta_a \tag{21}$$

where β_a and γ_a are considered as two small value constants and for all t ≥ 0, β_a may contains all possible existence of the bounded disturbance of the output.

The following theorem ensures the stability of adaptive system in presence of parameters uncertainties: It is assumed that the trajectories of the adaptive system are continuous with respect to **t**. If w_m is Persistently Exciting. Then for x_0, γ_a, β_a are small values, the state trajectories of adaptive system are bounded.

Proof: Let T > 0 such that $x(t) \leq h$ for $t \in [0, 1]$, and considering $n = H_a.u$ with assumption of:

$$\|n(t)\|_\infty \leq \gamma_a \|u(t)\|_\infty + \beta_a \tag{22}$$

For $t \in [0,T]$, and by Eq. (17)

$$u = \theta^T \cdot w = \left(\theta^{*T} + \emptyset^T\right) \cdot w = \theta^{*T} w_m + \theta^{*T} Qe + \theta^{*T} q_n n + \emptyset^T w_m + \emptyset^T Qe + \emptyset^T q_n n \tag{23}$$

and $\theta^T = \begin{bmatrix} c_0 & d_0 \end{bmatrix}$.

where $x \in B_h$, there are $\gamma_u, \beta_u \geq 0$ so,

$$\|u(t)\|_\infty \leq \gamma_u \|n(t)\|_\infty + \beta_u \tag{24}$$

For $t \in [0,T]$, and considering γ_a, β_a are small values, so

$$\gamma_a \gamma_u < 1 \text{and} \frac{\beta_a + \gamma_a \beta_u}{1 - \gamma_a \gamma_u} < c_n \tag{25}$$

where c_n is assumed as a constant.

Since β_a, γ_u, γ_a, and β_u are independent from T, $|x(t)| < h$ for over the time period. In addition, a value of T > 0, can be exist as $|x(t)| \leq h$ for $t \in [0,T]$ and $x(T) = h$, and this will be applied for $x(T) < h$.

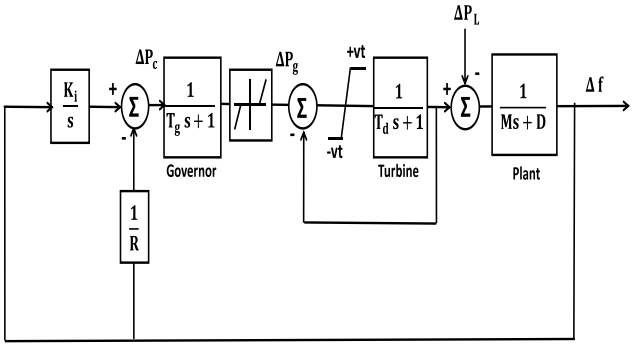

FIGURE 9. Block diagram of single area MG model.

VI. MICRO-GRID SYSTEM APPLICATION

The general block diagram of single area non-reheated turbine micro-grid (MG) is shown in Fig. 9. The mathematical model of the proposed micro-grid is described as follow [2]:

The frequency deviation ($\frac{df}{dt}$) can be expressed as:

$$\dot{\Delta f} = \left(\frac{1}{M}\right) \cdot \Delta P_d - \left(\frac{1}{M}\right) \cdot \Delta P_L - \left(\frac{D}{M}\right) \cdot \Delta f \tag{26}$$

The diesel generator dynamics can be expressed as:

$$\Delta \dot{P}_d = \left(\frac{1}{T_d}\right) \cdot \Delta P_g - \left(\frac{1}{T_d}\right) \cdot \Delta P_d \tag{27}$$

The governor dynamics can be expressed as:

$$\Delta \dot{P}_g = \left(\frac{1}{T_g}\right) \cdot \Delta P_c - \left(\frac{1}{R.T_g}\right) \cdot \Delta f - \left(\frac{1}{T_g}\right) \cdot \Delta P_g \tag{28}$$

where ($\Delta \dot{f}$, $\Delta \dot{P}_d$, $\Delta \dot{P}_g$) equal to ($\frac{df}{dt}$, $\frac{dP_d}{dt}$, $\frac{dP_g}{dt}$) respectively. While, Fig. 10 shows a general construction of MG.

VII. WCA BASED ADAPTIVE FREQUENCY CONTROL

WCA has been used as adaptive controller in [19]–[23], where the frequency deviation is the only signal used to feed the WCA as a guide to tune the gain of integral controller. The desired objective function of WCA is a function of the on-time value of Ki and the nominal system transfer function G_0 (S).

The model of the single area non-reheated turbine micro-grid linked with WCA is shown in Fig. 11.

A. WCA WITHOUT BALLOON EFFECT

Fig. 12 illustrates the simplified dynamic model of the single area power system used to drive the objective function of WCA; the closed loop second order system can be described as:

$$T.F = \frac{\omega_n^2}{S^{2+2\eta\omega_n S+\omega_n^2}} = \frac{\frac{k_i}{M_o}}{S^2 + \left(\frac{\left(D_o + \frac{1}{R_o}\right)}{M_o}\right) S + \frac{k_i}{M_o}} \tag{29}$$

where R_o, D_o and M_0 are the nominal values of R, D and M respectively. From (29):

$$\omega_n = \sqrt{k_i / M_o} \tag{30}$$

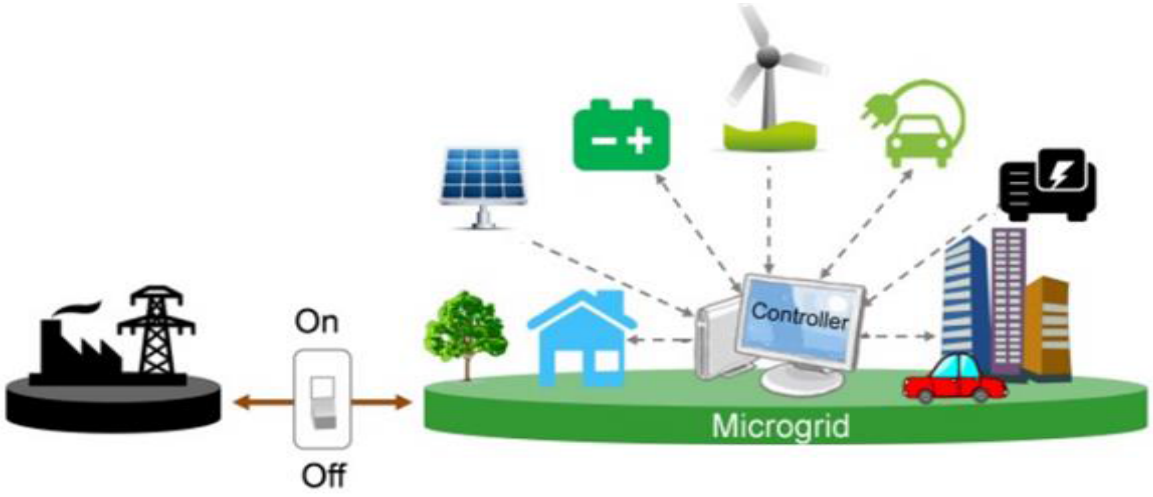

FIGURE 10. General construction of Micro-grid.

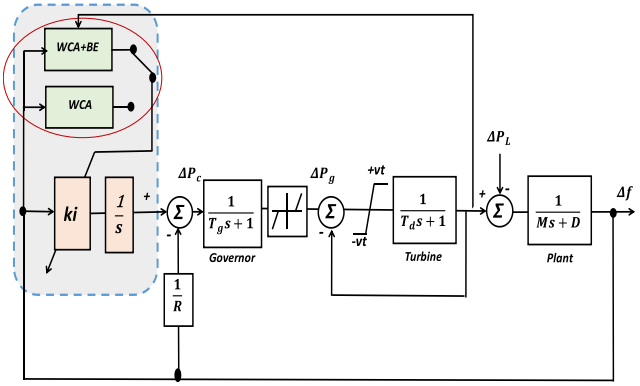

FIGURE 11. General block diagram model of isolated MG using WCA with/without BE.

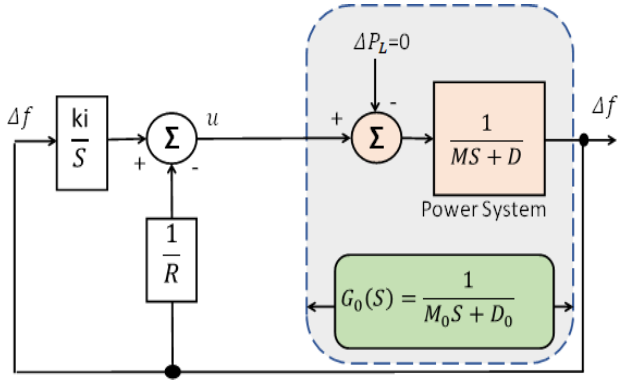

FIGURE 12. Dynamic model of a single-area micro-grid for a controlled area.

$$\eta = \frac{\left(\frac{\left(D_o+\frac{1}{R_o}\right)}{M_o}\right)}{2.\omega_n} \tag{31}$$

$$M_P = e^{\frac{-\pi\eta}{\sqrt{(1-\eta^2)}}} = e^{\frac{-\pi\left(D_o+\frac{1}{R_o}\right)}{2M_o\omega_n*\sqrt{\left(1-\left(\frac{\left(\left(D_o+\frac{1}{R_o}\right)\right)}{2.M_o\omega_n}\right)^2\right)}}} \tag{32}$$

$$T_s = \frac{4}{\omega_n.\eta} = \frac{8}{\left(\frac{\left(D_o+\frac{1}{R_o}\right)}{M_o}\right)} \tag{33}$$

$$T_r = \frac{\pi - \sqrt{(1-\eta^2)}}{\omega_n.\sqrt{(1-\eta^2)}} = \frac{\pi - \left(1 - \left(\frac{\left(\frac{\left(D_o+\frac{1}{R_o}\right)}{M_o}\right)}{2.\omega_n}\right)^2\right)^{0.5}}{\omega_n.\left(1 - \left(\frac{\left(\frac{\left(D_o+\frac{1}{R_o}\right)}{M_o}\right)}{2.\omega_n}\right)^2\right)^{0.5}} \tag{34}$$

The desired objective function is:

$$J = min \sum (T_r + T_s + M_P) \tag{35}$$

It can be noted that any system changes at any moment i, has no effect on the objective function, and this means that WCA will not deal with these changes effectively.

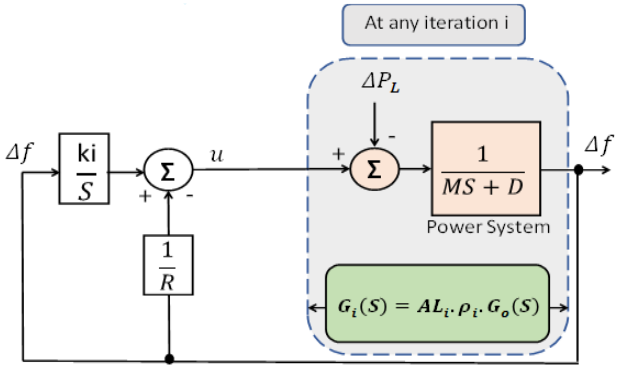

FIGURE 13. Reduced MG model controlled by WCA based BE.

B. WCA WITH BALLOON EFFECT

Fig. 13 illustrates the simple model of the studied micro-grid; this model has been used to drive objective function of WCA supported with Balloon Effect (BE):

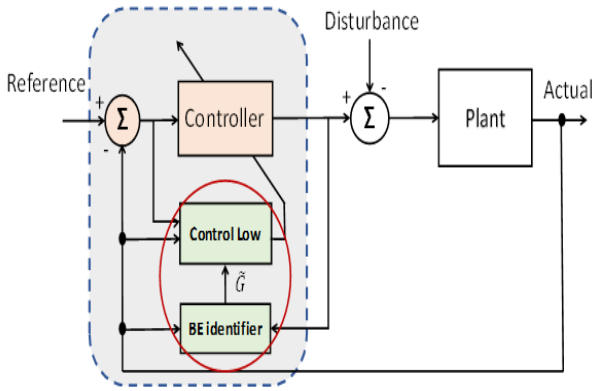

FIGURE 14. Model of adaptive control using balloon effect identifier.

at any iteration i, from Eq. (15):

$$G_i(S) = AL_i.\rho_i \cdot G_o(S)$$

where

$$G_o(S) = \frac{1}{M_o S + D_o} \tag{36}$$

So, the closed loop transfer function at any iteration i can be calculated as:

$$T.F = \frac{\omega_n^2}{S^{2+2\eta\omega_n S+\omega_n^2}} = \frac{\left(\frac{k_i.AL_i.\rho_i}{M_o}\right)}{S^2 + \left(\frac{\left(D_o+\frac{AL_i.\rho_i}{R_o}\right)}{M_o}\right)S + \left(\frac{k_i.AL_i.\rho_i}{M_o}\right)} \tag{37}$$

Then

$$\omega_n = \sqrt{\left(\frac{k_i.AL_i.\rho_i}{M_o}\right)},\ and\ \eta = \frac{\left(\frac{\left(D_o+\frac{AL_i.\rho_i}{R_o}\right)}{M_o}\right)}{2.\omega_n} \tag{38}$$

It is clear now that the objective function **J** at any iteration i is a function in k_i, AL_i and $\rho_{i..}$ Previous equations clarify that system changes such as parameters variations or load change will immediately affect on value of AL_i and the objective function at same time and this leads to increase the ability of WCA to deal with the system problems effectively.

According to the ''certainty equivalence controller'' [32], the control input can be calculated as:

$$U(S) = \left(\frac{K_i}{S + K_i\tilde{G}}\right)R(S) \tag{39}$$

For a discrete time domain:

$$U(k) = f(\tilde{G}(k), R(k+d)) \tag{40}$$

where $d \geq 1$ represents the time delay between the output and input. The control sequence of proposed WCA based BE is illustrated in Fig. 14.

VIII. RESULTS AND DISCUSSION

The suggested modified technique (WCA + BE) is used to tune LFC controller of small isolated power system. Matlab/Simulink environment is used for the simulation tests. The proposed micro-grid contains 20MW diesel generator is shown in Fig. 9. System nominal parameters and WCA parameters are listed in the following Table 1 and 2 respectively:

TABLE 1. Parameters of the studied micro-grid.

D	H = (M/2)	R	T_g	T_d
0.12	0.10	2.4	0.14	7

TABLE 2. Suggested parameters of WCA optimizer.

Candidate Solutions	**5**
Number of Rivers (Nsr)	9
Number of Generations	20
Distance between a river and sea	< dmax = $1e^{-16}$
The initial values of the design variable (Ki)	[0.05 0.15 0.2 0.1 0.33]

To validate the proposed adaptive integral controller adjusted by WCA based balloon effect, a system with the proposed controller has been tested under following cases:

A. FIRST CASE: PERFORMANCE EVALUATION UNDER 20% STEP LOAD PERTURBATION

In this case, the system has been exposed to step load demand at nominal system parameters. The load is stepped from 0 pu to 0.02 pu at t = 3 sec. GRC of the turbine, and dead-band of the governor are considered, 10% /minute for GRC and the maximum value of dead band for governor is chosen to be 0.05 pu.

To evaluate the WCA based BE for adaptive control scheme, a comparison was done to system with particle swarm (PSO) and classic WCA. Parameters of the PSO are listed in the following Table 3. Fig. 15 shows both of the frequency change and output power change of the diesel generator for the system with fixed integral controller, adaptive controller tuned using WCA, adaptive controller tuned using PSO, and adaptive controller tuned using WCA based BE. From this figure, it is clear that, system with adaptive controller tuned by WCA based BE gives the best power and frequency, it has no overshoot, and the smallest settling time. In addition, all of the adaptive controllers give better than the fixed parameters controller.

TABLE 3. Pso initial parameters values.

Swarm size	5.0
Inertia Weight (w)	9.0
Inertia weight damping ratio (w_{damp})	0.99
Personal Learning Coefficient (C1)	1.50
Global Learning Coefficient(C2)	2.0
Max. Iterations	100

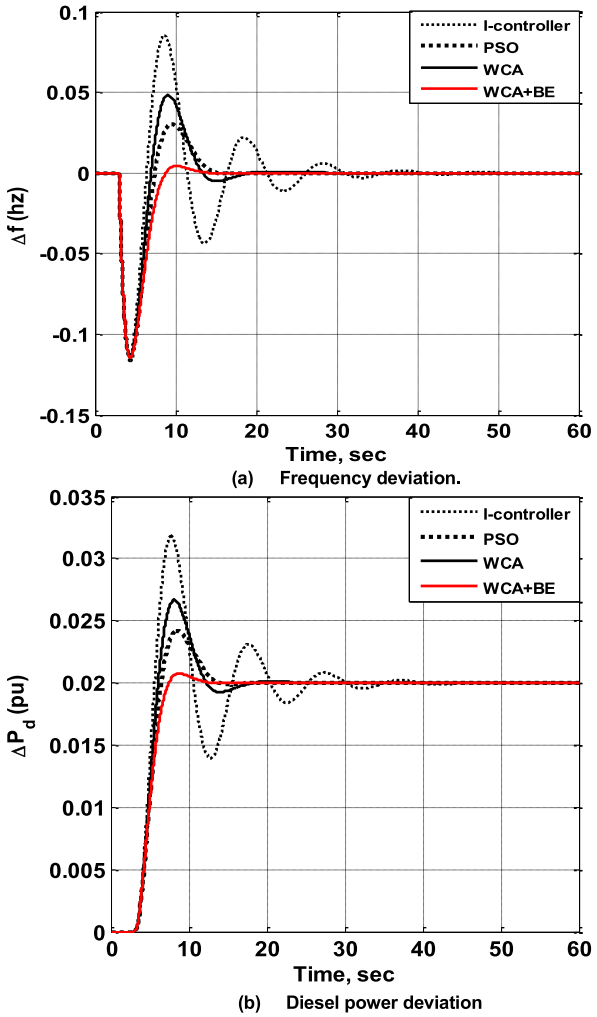

FIGURE 15. System response for case 1.

Fig. 16 illustrates the efforts of WCA based BE, it can be noted that it exerted much effort to enhance the total system response.

The Performance specifications (over shoot, under shoot and the settling time) of the adaptive WCA, PSO and conventional integrator controllers have been compared in Table 4.

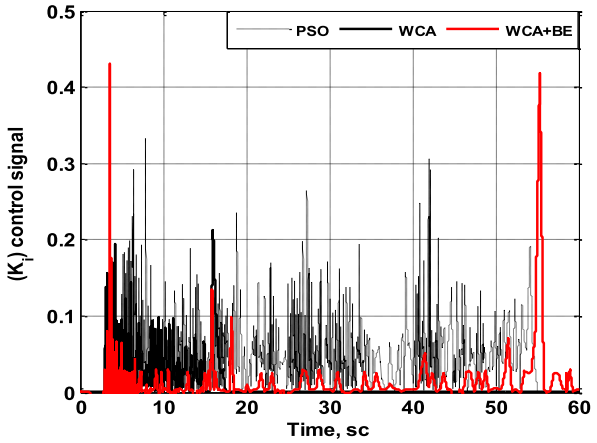

FIGURE 16. (Ki) output control signal for PSO and WCA, and WCA +BE optimizers.

TABLE 4. Performance specification due to 20% step load change.

Type of adaptive controller	Δf			ΔP_d	
	Over shoot	Under shoot	Settling time	Over shoot	Settling time
I-conventional	0.0781	-0.1203	35.123	0.0323	33.869
PSO	0.0275	-0.1202	18.176	0.0252	17.841
WCA	0.0495	-0.1202	15.022	0.0241	14.140
WCA based BE	0.0005	-0.1184	11.601	0.0208	10.285

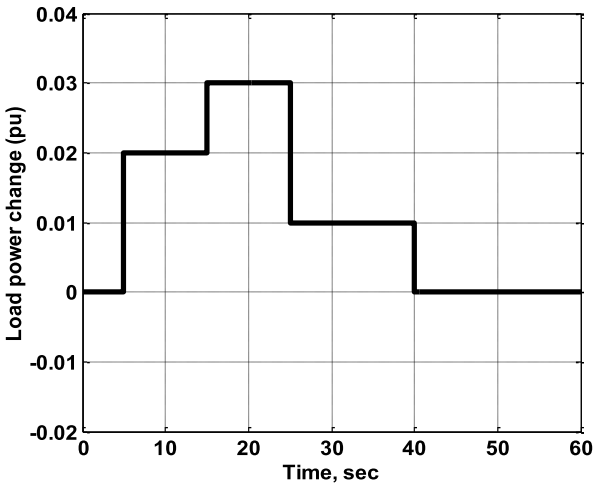

FIGURE 17. Load variations for case 2.

B. SECOND CASE: PERFORMANCE EVALUATION UNDER VARIABLE LOAD DISTURBANCES

To check the system with the proposed WCA based BE in difficult situations, it has been tested in the presence of system parameters changes (D is minimized to the value of 0.08 pu MW/Hz) at random load shown in Fig. 17.

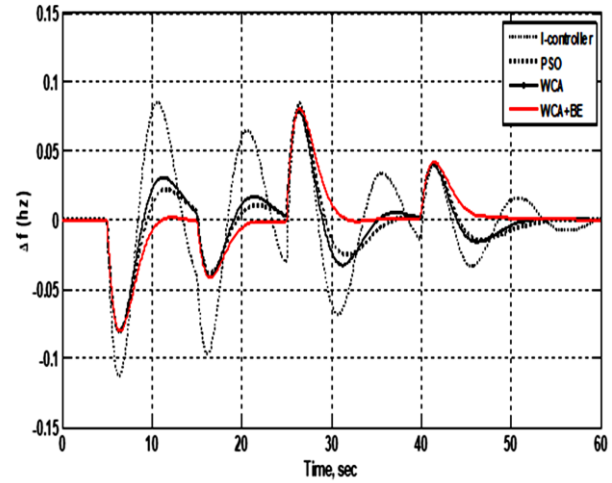

(a) Frequency deviation.

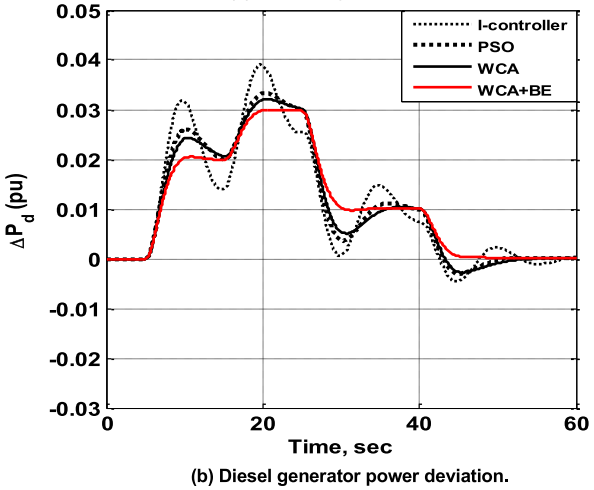

(b) Diesel generator power deviation.

FIGURE 18. System response for case 2.

Fig. 18 shows the system response obtained using the past types of controllers. It depicts that the frequency response in case of classical integral controller is very bad in case of load demand and system parameter uncertainty, but system with integral controller tuned by only WCA or WCA + BE can deal with this sever case efficiently. In addition, the system with suggested control method can give the best performance with minimum overshoot and smallest settling time.

IX. WCA + BE BASED POSITION CONTROL OF A DC MOTOR APPLICATION

A. POSITION-VELOCITY (PV) CONTROL OF DC MOTOR

The DC motor has several advantages such as the good relation between torque or speed and armature current, and the relation between the speed and the torque. DC motor is widely used in industrial applications such as robot, electric cars, and electric traction. Many different controllers for DC motor are introduced in [33]–[36].

To assure the effectiveness of the proposed WCA + BE, it has been applied to the position control of a cart driven by

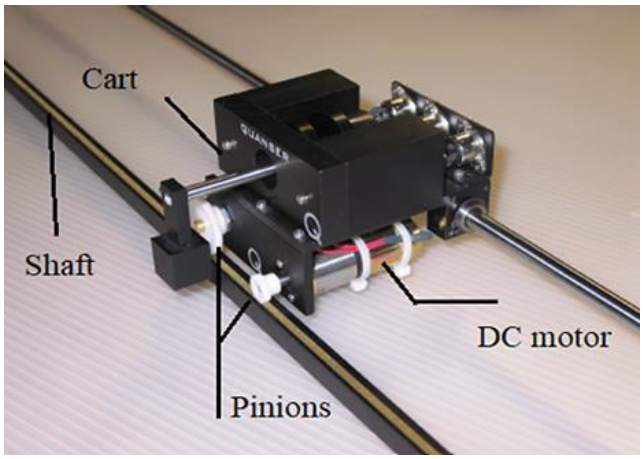

FIGURE 19. Studied cart moved by DC motor.

an armature-controlled DC motor shown in Fig. 19. The car consists of a movable aluminum mass, which moves linearly on a shaft with linear bearing, and this mass is driven by a DC motor at track with pinion mechanism in line with a planetary gearbox [37], [38]. The transfer function of the car system can be expressed as:

$$G(S) = \frac{X(S)}{V_m(S)} \tag{41}$$

In addition, by the second Newton's law:

$$M\left(\frac{d^2}{dt^2}x(t)\right) + F_{ai}(t) = F_c(t) - B_{eq}\left(\frac{d}{dt}x(t)\right) \tag{42}$$

The armature inertial torque F_{ai} can be represented as:

$$F_{ai} = \frac{\eta_g K_g T_{ai}}{r_{mp}} \tag{43}$$

Also using the second Newton's law on motion of the rotor shaft, it yields that:

$$J_m\left(\frac{d^2}{dt^2}\theta_m(t)\right) = T_{ai}(t) \tag{44}$$

The angular displacement θ_m can be calculated as:

$$\theta_m = \frac{K_g X}{r_{mp}} \tag{45}$$

The linear force Fc generated by the DC motor can be calculated by:

$$F_{ai} = \frac{\eta_g K_g T_m}{r_{mp}} \tag{46}$$

The generated torque by the DC motor can be expressed by:

$$T_m = \eta_m K_t I_m \tag{47}$$

while, the motor angular velocity can be calculated as:

$$\omega_m = \frac{K_g\left(\frac{d}{dt}X(t)\right)}{r_{mp}} \tag{48}$$

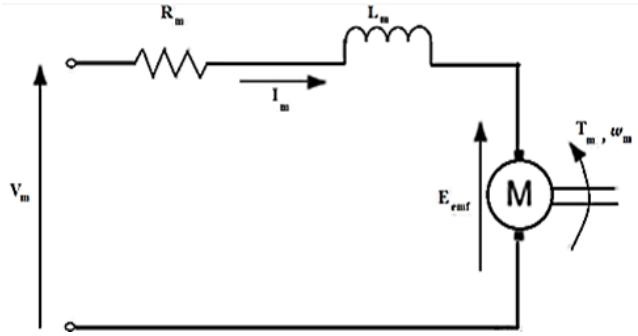

FIGURE 20. Electric circuit diagram of the armature circuit of the DC motor.

According to Fig. 20, and using Kirchhoff's voltage:

$$V_m - R_m I_m - L_m \left(\frac{d}{dt} I_m\right) - E_{emf} = 0 \tag{49}$$

By neglecting the motor inductance Im can be calculated as:

$$I_m = \frac{V_m - E_{emf}}{R_m} \tag{50}$$

The transfer function of the motor can be expressed as:

$$G(S) = \frac{r_{mp}\eta_g K_g \eta_m K_t}{\left(R_m M r_{mp}^2 + R_m \eta_g K_g^2 J_m\right)S^2 + \left(\eta_g K_g^2 \eta_m K_t K_m + B_{eq} R_m r_{mp}^2\right)S} \tag{51}$$

Fig. 21 illustrates the detailed block diagram of the proposed system and Table 5 shows the value of the system parameters. In addition, the maximum values of electrical motor are shown in Table 6.

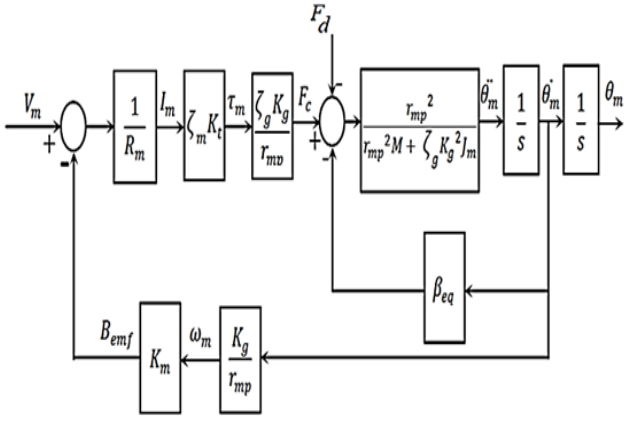

FIGURE 21. Block diagram model of the used DC motor.

Fig. 22 shows the block diagram of the proposed system with Position-Velocity (PV) controller. Nominal values of *Kp, Kv are:* $Kp_0 = 274.62$ *v/m and* $Kv_0 = 5.532$ *v.sec/m*, these values are designed to guide the system to give characteristics of 0.15 sec rise time and 10% overshoot. WCA + BE has been designed to tune the gains of the PV controller.

TABLE 5. The system item values.

Parameter	Values	Parameter	Values
ζg	100%	rmp	$6.35*10^{-3}$ M
ζm	100%	Kg	3.71
kt	7.67*10-3 N.m/A	Rm	2.6 ohms
M	0.97 Kg	Jm	$3.9*10^{-7}$ Kg.m^2

TABLE 6. Maximum electrical motor values.

Symbol	Max. Values
V	6 v
F	50 Hz
I	1 A
Ω	628.3 rad/sec

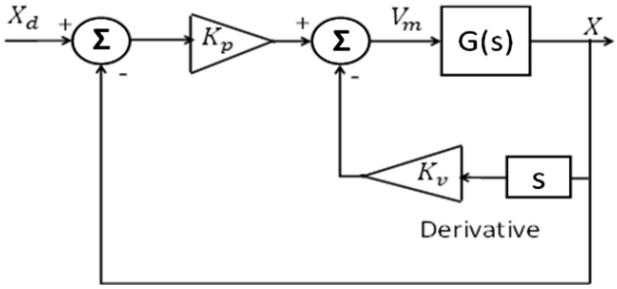

FIGURE 22. Block diagram of PV based position control of DC motor.

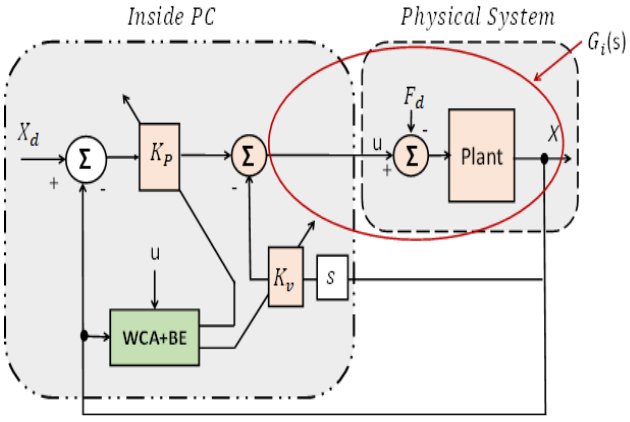

FIGURE 23. Block diagram for complete system with modified (WCA + BE).

B. ADAPTIVE PV CONTROLLER TUNED BY WCA + BE

Fig. 23 illustrates an adaptive position control system using the proposed WCA based BE. At any iteration, the total closed loop transfer function of the system can calculated as (52), shown at the bottom of the next page.

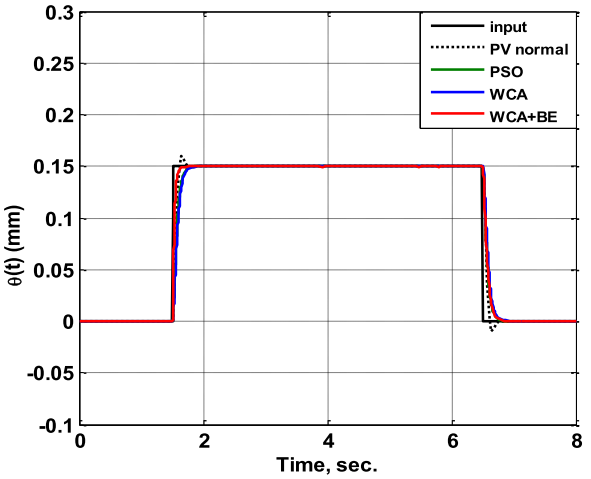

FIGURE 24. System position response.

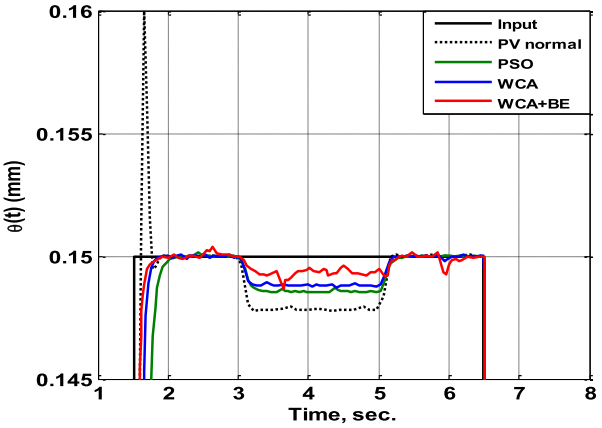

FIGURE 25. Focusing on period of load disturbance.

Where:

$$\omega_{ni} = \sqrt{2.46 * (\prod_{n=1}^{i} AL_n) * K_{pi}},\ and$$

$$\eta_i = \frac{\left(17.13 + 2.46{*}K_{vi} * \left(\prod_{n=1}^{i} AL_n\right)\right)}{2 * \omega_{ni}} \tag{53}$$

The objective function of WCA based BE is chosen as the same as in Eq. (29). It is clear that, at any iteration, J_{min} is a function in both of the values of K_{pi}, K_{vi} and the value of $(\prod_{n=1}^{i} AL_n)$. The modified WCA based BE technique has been designed with the following parameters:

Kp (initial values) = [200,210,220,230,440].

Kv (initial values) = [5, 10, 15, 20, 25].

The system with controller tuned by WCA based BE is compared with the system with that one tuned by classical WCA, PSO, and fixed parameters PV controller. Those four systems have been examined at step input change and step load disturbance as shown in Fig. 24. The step load started at t = 3sec. and finished at t = 5sec. with value of 0.2 N. The reference motor position signal is chosen to start at t = 1.5 sec by amplitude of 15 mm and finished at t = 4.5 sec.

It can be noted that the system with adaptive controllers have no overshoots, while system with WCA + BE can give best response with shortest rise-time. In addition, as shown in Fig. 25, the system with proposed adaptive control scheme can deal effectively with load disturbance problem.

NOMENCLATURE

Δf	Frequency deviation (Hz)
ΔP_g	Change in governor output
ΔP_d	Change in diesel mechanical power
ΔP_c	Change in speed changer position
ΔP_L	Change in demand load
D	Equivalent damping coefficient (pu/Hz)
H	Inertia constant (pu.sec)
R	Speed regulation characteristic (Hz/pu)
X(s)	The position of car
$V_m(s)$	Motor voltage
I_m	Motor current
Rm	Electric resistance of motor
L_m	Inductance of motor
E_{emf}	Back-Electromotive Force voltage
k_t	Motor torque constant
M	The total mass of car system
T_d	Diesel Time constant of (sec)
T_g	Governor Time constant (sec)
$T_{\Re}$	Rise Time constant (sec)
T_s	Settling time
M_p	Maximum overshoot
ζ_g	Efficiency of gearbox
rmp	Eotor pinion radius
kg	Planetary gearbox ratio
T_{ai}	Armature inertial torque
J_m	Rotor moment of inertia
ζ_m	Efficiency of motor.
F_{ai}	Armature rotational inertial force
F_c	Car driving force produced by the motor
B_{eq}	Equivalent viscous damping coefficient

$$\frac{X_i}{X_{di}} = \frac{2.46 * (\prod_{n=1}^{i} AL_n) * K_{pi}}{S^2 + \left(17.13 + 2.46{*}K_{vi} * \left(\prod_{n=1}^{i} AL_n\right)\right) S + (2.46 * K_{pi} * \left(\prod_{n=1}^{i} AL_n\right))} \tag{52}$$

X. CONCLUSION

This paper suggests a novel adaptive controller using modified water cycle algorithm that is used individually to tune the gains of the traditional controller parameters. In this paper, the normal WCA was adjusted by a new modification approach called 'Balloon Effect (BE)'. The main idea of BE is to make the objective function of WCA as a function of both of the values of tuned gains parameters and the value of system changes represented in a parameter called ($\mathbf{AL_i}$), This will increase the sensitivity of WCA to the load disturbance and system parameters uncertainties, and this will affect positively on the general characteristics of the system. Robustness and stability of proposed control scheme have been proven.

Adaptive controller using the proposed modified WCA algorithm has been applied to two different electrical systems: frequency control of micro-grid system and position control of a DC motor system, and the simulation results proved the efficiency of the proposed controller in both systems. The system with WCA based balloon effect has been compared with such systems as classical WCA, PSO and fixed parameters controllers in presence of load disturbance and system parameters variations. Simulation results assured the priority of the WCA + BE in all test cases.

For further study, Balloon Effect (BE) control design will be expanded to stabilize the oscillations in frequency and power with the integration of renewable energy sources such as PVs and wind energy in multi-area interconnected power systems. In addition, applying BE to other heuristics and meta-heuristics optimization techniques such as Electro-search, Ant-colony, Dragonfly, Particle swarm,...etc.

REFERENCES

[1] A. Dubey and P. Bondriya, "Literature survey on load frequency controller," *Int. J. Eng. Technol.*, vol. 3, no. 5, pp. 1604–1611, 2016.
[2] H. Bevrani, *Robust Power System Frequency Control* (Power Electronics and Power Systems). Springer, 2009.
[3] B. H. Abed-Alguni, "Island-based cuckoo search with highly disruptive polynomial mutation," *Int. J. Artif. Intell.*, vol. 17, no. 1, pp. 57–82, 2019.
[4] Y. Xu, C. Li, Z. Wang, N. Zhang, and B. Peng, "Load frequency control of a novel renewable energy integrated micro-grid containing pumped hydropower energy storage," *IEEE Access*, vol. 6, pp. 29067–29077, 2018.
[5] M. W. Siti, D. H. Tungadio, Y. Sun, N. T. Mbungu, and R. Tiako, "Optimal frequency deviations control in microgrid interconnected systems," *IET Renew. Power Gener.*, vol. 13, no. 13, pp. 2376–2382, Oct. 2019.
[6] S. Kayalvizhi and D. M. Vinod Kumar, "Load frequency control of an isolated micro grid using fuzzy adaptive model predictive control," *IEEE Access*, vol. 5, pp. 16241–16251, 2017.
[7] M. I. Mosaad and F. Salem, "LFC based adaptive PID controller using ANN and ANFIS techniques," *J. Electr. Syst. Inf. Technol.*, vol. 1, no. 3, pp. 212–222, Dec. 2014.
[8] H. Shayeghi, H. A. Shayanfar, and A. Jalili, "Load frequency control strategies: A state-of-the-art survey for the researcher," *Energy Convers. Manage.*, vol. 50, no. 2, pp. 344–353, Feb. 2009.
[9] T. Senjyu, M. Tokudome, A. Yona, H. Sekine, T. Funabashi, and C.-H. Kim, "A frequency control approach by decentralized generators and loads in power systems," in *Proc. IEEE 2nd Int. Power Energy Conf.*, Dec. 2008, pp. 79–84.
[10] D. K. Sambariya and S. Shrangi, "Optimal design of PID controller for load frequency control using harmony search algorithm," *Indonesian J. Electr. Eng. Comput. Sci.*, vol. 5, no. 1, pp. 19–32, 2017.
[11] B. K. Sahu, T. K. Pati, J. R. Nayak, S. Panda, and S. K. Kar, "A novel hybrid LUS–TLBO optimized fuzzy-PID controller for load frequency control of multi-source power system," *Int. J. Electr. Power Energy Syst.*, vol. 74, pp. 58–69, Jan. 2016.
[12] R. K. Sahu, S. Panda, and S. Padhan, "A hybrid firefly algorithm and pattern search technique for automatic generation control of multi area power systems," *Int. J. Elect. Power Energy Syst.*, vol. 64, pp. 9–23, Jan. 2015.
[13] H. Gozde, M. C. Taplamacioglu, and I. Kocaarslan, "Comparative performance analysis of artificial bee colony algorithm in automatic generation control for interconnected reheat thermal power system," *Int. J. Electr. Power Energy Syst.*, vol. 42, no. 1, pp. 167–178, Nov. 2012.
[14] S. Duman, N. Yorukeren, and I. H. Altas, "Load frequency control of a single area power system using gravitational search algorithm," in *Proc. Int. Symp. Innov. Intell. Syst. Appl.*, Jul. 2012, pp. 1–5.
[15] M. Č. Bošković, T. B. Šekara, and M. R. Rapaić, "Novel tuning rules for PIDC and PID load frequency controllers considering robustness and sensitivity to measurement noise," *Int. J. Electr. Power Energy Syst.*, vol. 114, Jan. 2020, Art. no. 105416.
[16] S. M. Abd-Elazim and E. S. Ali, "Load frequency controller design via BAT algorithm for nonlinear interconnected power system," *Int. J. Electr. Power Energy Syst.*, vol. 77, pp. 166–177, May 2016.
[17] M. Gheisarnejad and M. H. Khooban, "Secondary load frequency control for multi-microgrids: HiL real-time simulation," *Soft Comput.*, vol. 23, no. 14, pp. 5785–5798, Jul. 2019.
[18] M. H. Khooban, A. Alfi, and D. N. M. Abadi, "Control of a class of nonlinear uncertain chaotic systems via an optimal type-2 fuzzy proportional integral derivative controller," *IET Sci., Meas. Technol.*, vol. 7, no. 1, pp. 50–58, Jan. 2013.
[19] H. M. Hasanien, "Transient stability augmentation of a wave energy conversion system using a water cycle algorithm-based multiobjective optimal control strategy," *IEEE Trans. Ind. Informat.*, vol. 15, no. 6, pp. 3411–3419, Jun. 2019.
[20] A. Latif, D. C. Das, S. Ranjan, and A. K. Barik, "Comparative performance evaluation of WCA-optimised non-integer controller employed with WPG–DSPG–PHEV based isolated two-area interconnected microgrid system," *IET Renew. Power Gener.*, vol. 13, no. 5, pp. 725–736, Apr. 2019.
[21] Y. Xu and Y. Mei, "A modified water cycle algorithm for long-term multi-reservoir optimization," *Appl. Soft Comput.*, vol. 71, pp. 317–332, Oct. 2018.
[22] H. M. Hasanien and M. Matar, "Water cycle algorithm-based optimal control strategy for efficient operation of an autonomous microgrid," *IET Gener., Transmiss. Distrib.*, vol. 12, no. 21, pp. 5739–5746, Nov. 2018.
[23] H. Eskandar, A. Sadollah, A. Bahreininejad, and M. Hamdi, "Water cycle algorithm—A novel Metaheuristic optimization method for solving constrained engineering optimization problems," *Comput. Struct.*, vols. 110–111, pp. 151–166, Nov. 2012.
[24] P. Purey, A. Technical Campus, and R. Arya, "Application of jaya algorithm for reactive power reserve optimization accounting constraints on voltage stability margin," *Int. J. Eng. Trends Technol.*, vol. 51, no. 2, pp. 106–114, Sep. 2017.
[25] M.-H. Khooban, T. Niknam, F. Blaabjerg, P. Davari, and T. Dragicevic, "A robust adaptive load frequency control for micro-grids," *ISA Trans.*, vol. 65, pp. 220–229, Nov. 2016.
[26] T. Hassan Mohamed and M. M. Hussein, "Online gain tuning of conventional load frequency controller for microgrid power system," in *Proc. 20th Int. Middle East Power Syst. Conf. (MEPCON)*, Dec. 2018, pp. 424–428.
[27] C. Wadhwa, "Load frequency control of single area power system using JAYA algorithm," *Int. Res. J. Eng. Technol.*, vol. 4, no. 7, pp. 2106–2110, Jul. 2007.
[28] T. H. Mohamed, H. Abubakr, M. M. Hussein, and G. Shabib, "Load frequency controller based on particle swarm optimization for isolated microgird system," *Int. J. Appl. Energy Syst.*, vol. 1, no. 2, pp. 69–75, 2019.
[29] M. P. Bendsøe and O. Sigmund, *Topology Optimization: Theory, Methods, and Applications*. Berlin, Germany: Springer, 2003.
[30] M. R. Bonyadi and Z. Michalewicz, "Analysis of stability, local convergence, and transformation sensitivity of a variant of the particle swarm optimization algorithm," *IEEE Trans. Evol. Comput.*, vol. 20, no. 3, pp. 370–385, Jun. 2016.
[31] S. Sastry and M. Bodson, *Adaptive Control: Stability, Convergence, and Robustness*. Upper Saddle River, NJ, USA: Prentice-Hall, 1989.

[32] B. Bhushan and M. Singh, "Adaptive control of DC motor using bacterial foraging algorithm," *Appl. Soft Comput.*, vol. 11, no. 8, pp. 4913–4920, Dec. 2011.
[33] A. Fitzregerald, C. Kingsley, and S. Umans, *Electric Machinery*, 6th ed. New York, NY, USA: McGraw-Hill, 2005, pp. 357–406.
[34] P. Salawria, R. Lodhi, and P. Nema, "Different methods of speed control for brushless DC motor: A review," *Int. J. Emerg. Technol.*, vol. 8, no. 1, pp. 25–29, 2017.
[35] K. Sailan and K. D. Kuhnert, "DC motor angular position control using PID controller for the purpose of controlling the hydraulic pump," in *Proc. Int. Conf. Control, Eng. Inf. Technol. (CEIT)*, vol. 1, 2013, p. 22–26.
[36] R. Lu, S. Li, and L. Xue, "Robust H_∞ optimal speed control of DC motor using LMI approach," in *Proc. Chin. Control Decis. Conf.*, Jul. 2008, pp. 4350–4354.
[37] A. Abdulameer, M. Sulaiman, M. Aras, and D. Saleem, "Tuning methods of PID controller for DC motor speed control," *Indonesian J. Electr. Eng. Comput. Sci.*, vol. 3, no. 2, pp. 343–349, 2016.
[38] E. H. Abdelhameed, T. H. Mohamed, M. M. Hamed, and G. E.-S. Ahmed, "Fuzzy-based position-velocity controller gain scheduling for load disturbance rejection in a positioning servo system," in *Proc. 20th Int. Middle East Power Syst. Conf. (MEPCON)*, Dec. 2018, pp. 666–671.
[39] M. A. M. Alamin, T. H. Mohamed, and A. M. Hassan, "Position control of a cart moved by DC motor using PV-DFC method supported by balloon effect," *J. Int. J. Adv. Sci. Technol.*, vol. 29, no. 3, pp. 2207–2217, 2020.
[40] Y. A. Dahab, H. Abubakr, and T. H. Mohamed, "Adaptive load frequency control of power systems using electro-search optimization supported by the balloon effect," *IEEE Access*, vol. 8, pp. 7408–7422, 2020.

TAREK HASSAN MOHAMED was born in 1975. He received the B.Sc. degree in control engineering from Minoufta University, Egypt, in 2006, and the M.Sc. and Ph.D. degrees in electrical engineering from Minia University, Egypt, in 2012.

From 2006 to 2012, he was an Assistant Lecturer with the Faculty of Energy Engineering, Aswan University, Egypt. Since 2017, he has been an Assistant Professor with the Electrical Engineering Department, Faculty of Energy Engineering, Aswan University. Since 2018, he has been the Head of the Department. He is the author of more than 40 articles. His research interests include automatic control, power system control, and renewable energy.

HUSSEIN ABUBAKR was born in 1990. He received the Diploma degree in metals from the Industrial Technical Institute for Aluminum, in 2009, the B.Sc. and M.Sc. degrees in electrical power engineering from Aswan University, Egypt, in 2014 and 2019, respectively. From 2014 to 2016, he has worked as a Quality Control Engineer with the Electronic Construction Services Company, Cairo, Egypt. Since 2019, he has been working as an Assistant Lecturer with the Faculty of Energy Engineering, Aswan University. His research interests include power system control, optimization techniques, micro grids, and renewable energy sources.

MOHAMED ABDELHAMID MOHAMED ALAMIN received the B.Sc. and M.Sc. degrees in electrical engineering from Aswan University, Aswan, Egypt, in 2013 and 2019, respectively, where he is currently pursuing the Ph.D. degree in electrical engineering with the Faculty of Engineering. Since 2017, he has been an Electrical Engineer with Egyptian Hydro-Power Generation Company, Egypt. His research interest includes automatic control of servo motors.

AMMAR MOSTAFA HASSAN received the B.Sc. and M.Sc. degrees from Assiut University, Assiut, Egypt, in 1995 and 2005, respectively, and the Ph.D. degree from Minia University, Minia, Egypt, in 2012. He has spent two years at Otto-von-Guericke University, Magdeburg, Germany. He is currently the Head of the Computer Science Department, Arab Academy for Science, Technology and Maritime Transport, South Valley Branch, Aswan, Egypt. His research interests include image processing, image hashing, cryptography, automatic/digital control, and image authentication.